Optical and structural studies of compositional inhomogeneity in strain-relaxed indium gallium nitride films

LH Robins, JT Armstrong, RB Marinenko, MD Vaudin, CE Bouldin, JC Woicik, AJ Paul and WR Thurber

National Institute of Standards and Technology, Gaithersburg, MD 20899

KE Miyano

City University of New York, New York, NY 10031

CA Parker, JC Roberts, SM Bedair, EL Piner, MJ Reed, and NA El-Masry

North Carolina State University, Raleigh, North Carolina 27695-7911

SM Donovan and SJ Pearton

University of Florida, P.O. Box 116400, 132 Ritines Hall, Gainesville, Florida 32611

Abstract. The structural and optical properties of indium gallium nitride ($In_xGa_{1-x}N$) films with $0.04 < x < 0.47$, grown by metal-organic chemical vapor deposition, were examined by x-ray diffraction (XRD), extended x-ray absorption fine structure (EXAFS), optical transmittance, and cathodoluminescence (CL) spectroscopies. The average indium fraction (x_{avg}) was measured by wavelength-dispersive x-ray spectroscopy in an electron-probe microanalyzer (WDS/EPMA). Pure GaN and InN films were also characterized. Comparison of the 0006 XRD data with the WDS data shows that the lattice constant c is a linear function of x_{avg}. A small amount of a high-indium ($x \approx 0.99$) phase was observed in films with $x_{avg} \geq 0.44$. From EXAFS, the composition of the indium second-neighbor shell is equal (within the 2σ measurement uncertainty) to x_{avg}. These results are consistent with a random-alloy structure. The optical band gap, determined from the position of the absorption edge in the transmittance spectrum, and also from the highest-energy CL peak, is described well by a quadratic function of x_{avg} with a second-order (bowing) parameter of (-4.57 ± 0.75) eV. The magnitude of the composition fluctuations in the alloy films, denoted Δx, was estimated by analyzing the full widths at half maximum (FWHMs) of the XRD peaks and also the band-edge CL peaks. The two calculations of Δx give similar results.

1. Introduction

Recent advances in the growth of III-Nitride semiconductor films[1] have led to the development of high-efficiency, short-wavelength light-emitting diodes and laser diodes. The active layers of the light-emitting devices are usually composed of $In_xGa_{1-x}N$. Because of the 10% fractional difference

between the Ga-N and In-N bond lengths, phase separation and compositional inhomogeneity are common phenomena in $In_xGa_{1-x}N$ films. According to the modified valence-force-field model of Ho and Stringfellow[2], at 800 °C the miscibility gap of $In_xGa_{1-x}N$ is $0.06 < x < 0.94$, and spinodal decomposition occurs for $0.20 < x < 0.80$.

In prior experimental work, Osamura[3] observed phase separation by x-ray diffraction (XRD) in polycrystalline $In_xGa_{1-x}N$; Singh[4] observed phase separation by XRD in 0.3 µm to 0.4 µm thick molecular beam epitaxy (MBE) grown films with $x > 0.3$; and Piner[5] and El-Masry[6] observed phase separation by selected-area diffraction transmission electron microscopy (SAD-TEM) in 0.3 µm to 0.5 µm thick metal-organic chemical vapor deposition (MOCVD) grown films with $x > 0.25$. Piner and El-Masry also observed spinodal decomposition by TEM imaging in a film with $x \approx 0.45$.

In the present study, the structural and optical properties of a set of ≥ 0.38 µm thick $In_xGa_{1-x}N$ films with $0.04 \leq x \leq 0.47$ were examined by the following techniques: XRD θ-2θ scans and rocking curves (long-range structure), EXAFS (short-range structure), wavelength-dispersive spectroscopy in an electron-probe microanalyzer (WDS/EPMA) (composition), and optical transmittance and cathodoluminescence (CL) spectroscopies.

While the films in the present study and the studies cited above are thick enough to have bulk-like properties, the $In_xGa_{1-x}N$ active layers in light-emitting devices are usually quantum wells (1 nm to 5 nm thick). Although a discussion of the unique properties of $In_xGa_{1-x}N$ quantum wells is beyond the scope of this work, the effect of inhomogeneity and phase separation on the optical properties of quantum-well structures is currently an active area of research[7][8].

2. Experimental procedure

The $In_xGa_{1-x}N$ films examined in this study were grown by atmospheric-pressure MOCVD on (0001) sapphire substrates in a radio-frequency inductively heated vertical chamber (at North Carolina State University). In the earlier depositions (done in 1996), the buffer layer (between the substrate and the $In_xGa_{1-x}N$) was a 0.1 µm to 0.2 µm thick AlGaN graded to GaN layer grown at 950 °C; in the later depositions (1998 and 1999), the buffer layer was a 0.45 µm to 1.0 µm thick GaN layer grown at 1000 °C. A pure GaN film was grown by a similar process. A pure InN film was grown on an AlN nucleation layer by metal-organic molecular beam epitaxy (at the University of Florida).

The indium fraction in each $In_xGa_{1-x}N$ film was measured by WDS/EPMA with an incident electron energy of 8 keV. The In, Ga and N atomic concentrations were calibrated with InAs, GaP, and GaN standards respectively. At least five spots on each sample were probed by WDS. The best WDS estimate of the indium fraction is denoted x_{avg}.

The c-axis lattice constants of the $In_xGa_{1-x}N$, GaN, and InN layers were determined from θ-2θ scans of the high-angle, 0006 diffraction peaks. Indium K edge EXAFS of several $In_xGa_{1-x}N$ films was collected on beamline X23A2 at the National Synchrotron Light Source. The EXAFS data were analyzed using standard background removal and Fourier transform methods.

Transmittance spectra were obtained in a UV-to-near-IR (0.2 µm to 2.5 µm) spectrophotometer, and normalized to the transmittance of an uncoated sapphire substrate. Room-temperature CL spectra were obtained in a scanning electron microscope with beam voltage of 5 kV.

Additional details of the deposition processes and characterization techniques are given in a more extensive discussion of this work[9].
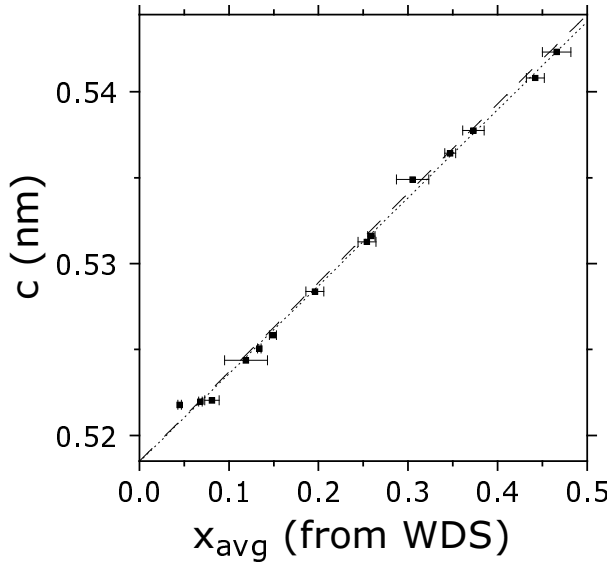
Fig. 1. Lattice constants c of In$_x$Ga$_{1-x}$N films as a function of composition x_{avg}. The dashed line is an interpolation between GaN and InN endpoints; the dotted line is a fit to the alloy data.
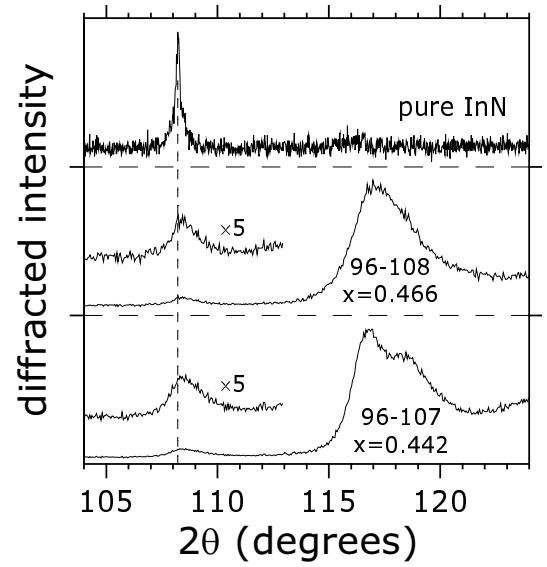

Fig. 2. XRD θ-2θ scans of InN and selected In$_x$Ga$_{1-x}$N films. Peaks ascribed to high-indium ($x \approx 0.99$) phases in alloy films are also shown on an expanded scale.

3. Results and discussion

3.1. *Structural characterization (WDS/EPMA, XRD, EXAFS)*

The lattice constant c, determined from the fitted peak diffraction angle (θ_{peak}) by the basic diffraction equation $c = n\lambda_{x\text{-}ray}/(2 \sin(\theta_{peak}))$ with n=6 and $\lambda_{x\text{-}ray}$=0.15406 nm, is plotted as a function of x_{avg} in Fig. 1. Vegard's law is seen to be obeyed; the lattice constants of the In$_x$Ga$_{1-x}$N films are fit well by a linear interpolation between the endpoint compounds, $c(x_{avg}) = c_{GaN}(1-x_{avg}) + c_{InN}x_{avg}$, with c_{GaN}=0.5185 nm[10] and c_{InN}=0.5705 nm[11]. In Fig. 1, the Vegard's law interpolation is shown as a dashed line, and, for comparison, an unconstrained linear fit to the alloy data is shown as a dotted line. The horizontal error bars in Fig. 1 represent the 2σ uncertainties of x_{avg} as estimated from the spot-to-spot variation of the WDS/EMPA results. (In this study, all measurement uncertainties are reported at the 2σ level.)

A second, high-indium phase was observed by XRD in the alloy films with x_{avg}>0.4. The θ-2θ scans for these samples and for the pure InN/sapphire sample are plotted in Fig. 2. The angular position of the high-indium peak in the alloy films is 108.4°, compared to 108.2° for pure InN. The composition of the second phase is thus estimated (from Vegard's law) to be x=0.99. The integrated intensity ratio of the x=0.99 peak to the dominant In$_x$Ga$_{1-x}$N peak in these films is <0.04.

Six In$_x$Ga$_{1-x}$N films were characterized by In K edge EXAFS. The In/(In+Ga) ratio in the indium second-neighbor shell, denoted $x_{N=2}$, was calculated by curve-fitting to the EXAFS radial distribution function. The EXAFS $x_{N=2}$ values are compared with the WDS/EPMA x_{avg} values in Fig. 3. Within the experimental uncertainty of the EXAFS results ($2\sigma(x_{N=2})$=0.05 to $2\sigma(x_{N=2})$=0.09), the composition of the indium second-neighbor shell cannot be distinguished from the average composition. In a previous EXAFS study of MBE-grown In$_x$Ga$_{1-x}$N films (growth temperature $\approx$ 400 °C), the In-Ga interatomic separations[12] determined from In edge EXAFS and from Ga edge EXAFS were found to be in good agreement with each other, as expected for a random alloy structure.
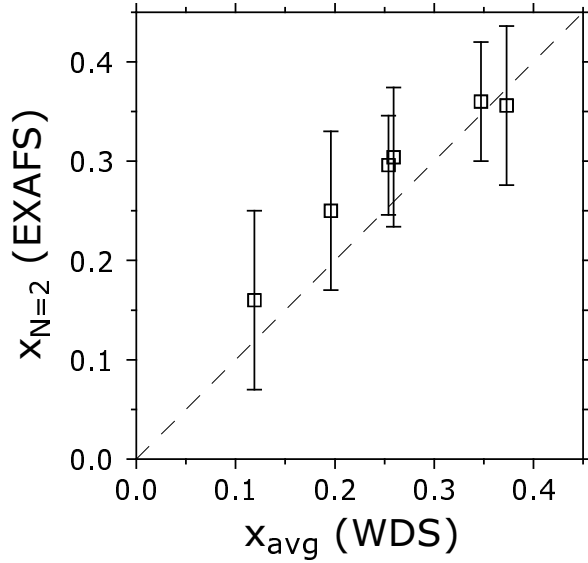
Fig. 3. Comparison of In/(In+Ga) ratio in the indium second-neighbor shell ($x_{N=2}$) from EXAFS, and average In/(In+Ga) ratio (x_{avg}) from WDS. Dashed line shows $x_{N=2} = x_{avg}$.
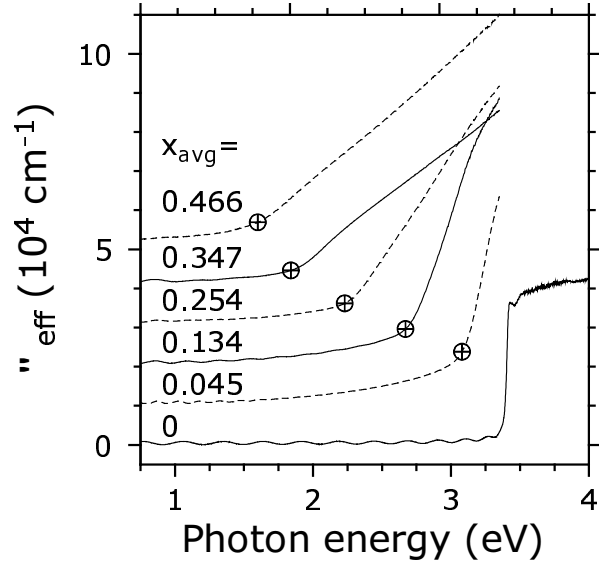
Fig. 4. Effective optical absorption coefficients, $\alpha_{eff}(E)$, of GaN and selected $In_xGa_{1-x}N$ films, from transmittance. Symbols (circles with cross-hairs) show estimated optical band gap energies.

If a large fraction of the indium atoms were located in indium-rich clusters, as proposed in some models[13], then the ratio of In-In to In-Ga pairs in the second shell would be larger than the average In/Ga ratio; i.e., $x_{N=2}-x_{avg}>0$. The absence of observable (by EXAFS) indium clustering is thus further evidence, in addition to the Vegard's law behavior of the c lattice constant (Fig. 1), that the In/Ga distribution in most films is random or nearly random. Because of the large uncertainties of the $x_{N=2}$ values calculated from EXAFS, however, indium clustering cannot be completely ruled out.

3.2. *Optical characterization (transmittance and CL)*

The measured optical transmittances were converted to absorption (cm^{-1}) units using the equation $\alpha_{eff}(E)=(1/d_f)\log(1/T(E))$, where T(E) is the transmittance and d_f is the $In_xGa_{1-x}N$ layer thickness. The parameter $\alpha_{eff}(E)$ includes reflection and scatter losses as well as true internal absorption. The $\alpha_{eff}(E)$ spectra of the pure GaN film and selected $In_xGa_{1-x}N$ films are plotted in Fig. 4. (The film thicknesses d_f were estimated from the spacing of interference fringes in the transmittance spectra, not shown.)

The pure GaN film shows a sharp absorption edge at 3.4 eV, as expected. In contrast, in the alloys, $\alpha_{eff}(E)$ shows an approximately linear increase with photon energy above a characteristic "turning point" energy, identified as the optical absorption band gap, $E_{G,abs}$. The value of $E_{G,abs}$ decreases with increasing x; the above-gap slope, $\partial\alpha_{eff}(E)/\partial E$, also decreases with increasing x. The band gap energies were quantified using an empirical criterion[14] related to the intuitive idea of a "turning point": $E_{G,abs}$ is taken to be the energy at which $\partial^2\ln(\alpha_{eff}(E))/\partial E^2$ is maximum. Numerical smoothing and differentiation was used to calculate the second derivative values from the data.

In each $In_xGa_{1-x}N$ film, the room-temperature CL spectrum (not shown here) contains two or more peaks[9]. The peak energies were determined by curve-fitting to a sum of Gaussians. The highest-energy CL peak in each sample correlates well with $E_{G,abs}$, and is thus ascribed to band-to-band (or near-band-edge impurity) recombination. The energy of the band-edge peak is denoted $E_{G,CL}$.

The transmittance ($E_{G,abs}$) and CL ($E_{G,CL}$) band gaps are plotted in Fig. 5. Three different
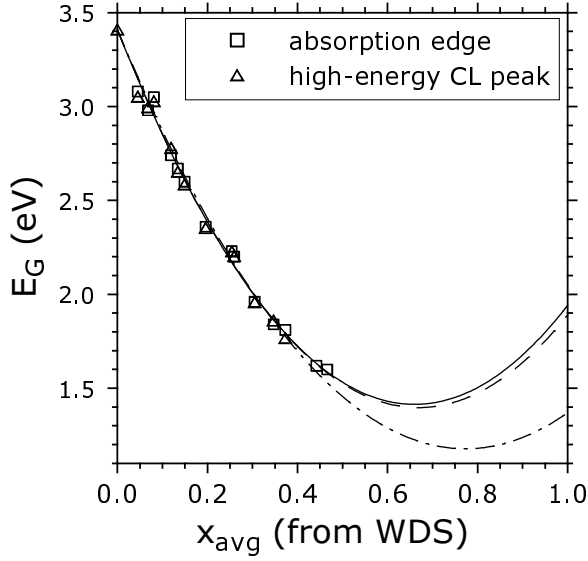
Fig. 5. Band gaps of $In_xGa_{1-x}N$ films from transmittance and CL. The dashed, dash-dotted and solid lines are quadratic fits with different constraints at $x_{avg}=1$, as discussed in the text.
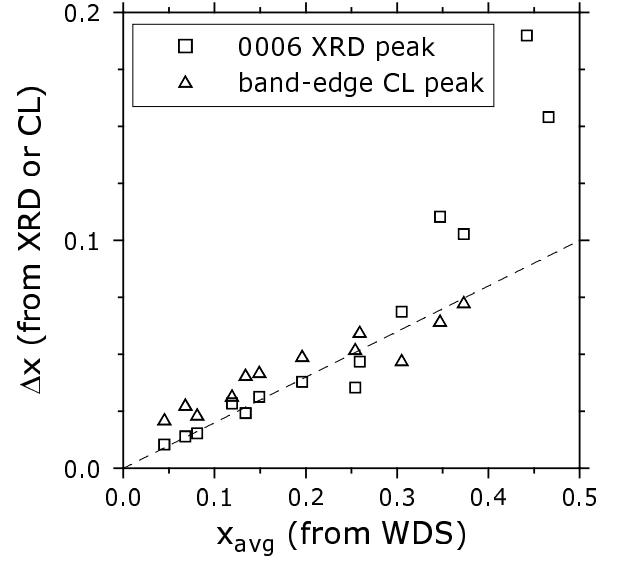
Fig. 6. Compositional inhomogeneity of $In_xGa_{1-x}N$ films (Δx), estimated from FWHMs of 0006 XRD peaks and, independently, from FWHMs of band-edge CL peaks.

quadratic fits to the data are shown in Fig. 5, all based on the function $E_G\{x_{avg}\} = E_{GaN}(1-x_{avg}) + E_{InN}(x_{avg}) + E_B(x_{avg})(1-x_{avg})$ with $E_{GaN}=3.41$ eV. The non-linear term, E_B, is usually called the bowing parameter. The fits differ only in the constraint on the InN ($x=1$) endpoint. In the first fit (dashed line), the endpoint is taken to be $E_{InN}=1.89$ eV, as reported in the literature[15]. In the second fit (dash-dotted line), the endpoint is taken to be $E_{InN}=1.37$ eV, as observed for the pure InN film in this study. (The 0.52 eV band gap reduction of our InN film, as compared to the literature value[15], is tentatively ascribed to band tailing due to deep defect or impurity levels. Hall effect measurements[9] provide evidence for a high density of deep levels in the InN film.) In the third fit (solid line), E_{InN} is unconstrained. The unconstrained fit is seen to agree better with the $E_{InN}=1.89$ eV fit than with the $E_{InN}=1.37$ eV fit. Note, however, that chi-squared is similar for all three fits. The parameter values for the unconstrained fit are $E_B=(-4.57\pm0.75)$ eV and $E_{InN}=(1.94\pm0.51)$ eV. The large uncertainties are due to the high degree of correlation of the two fitting parameters.

3.3. Estimates of compositional inhomogeneity from structural and optical data

If it is assumed that the full width at half maximum (FWHM) of the 0006 XRD peak arises primarily from variation of the c lattice constant, and the variation of c arises primarily from compositional fluctuations, then the magnitude of the compositional fluctuations, Δx, can be estimated from Vegard's law: $\Delta x_{XRD} = \Delta c/(c_{InN}-c_{GaN})$ where Δc is the XRD FWHM in lattice constant units. Similarly, if it is assumed that the FWHM of the band-edge CL peak arises primarily from compositional fluctuations, then Δx can be estimated by differentiation of the equation for $E_G\{x_{avg}\}$: $\Delta x_{CL} = \Delta E_{CL} / |E_{GaN} - E_{InN} - E_B + 2E_Bx_{avg}|$. The compositional inhomogeneities Δx_{XRD} and Δx_{CL}, estimated from the XRD and CL FWHMs respectively, are plotted in Fig. 6.

The values of Δx_{XRD} and Δx_{CL} are seen to be in good agreement with each other. Because the CL and XRD measurements are independent, this agreement supports the validity of both model calculations. The calculated values of Δx are close to $\Delta x=0.2x_{avg}$ (dashed line in Fig. 6) for $x_{avg}<0.35$.

4. Conclusion

The structural (XRD, EXAFS) and compositional (WDS/EPMA) characterization results suggest that the structure of the $In_xGa_{1-x}N$ films is well described by a random-alloy model, i.e. a random distribution of In and Ga atoms on the cation sublattice, except for the presence of a small amount of a high-indium second phase in the films with x_{avg}>0.4. Both optical transmittance and CL measurements show that the optical band gap varies as a quadratic function of x_{avg} with a bowing parameter (–4.57±0.75) eV. The magnitude of the compositional fluctuations in each alloy film, Δx, was estimated from a model calculation based on the FWHM of the 0006 XRD peak, and, independently, from a model calculation based on the FWHM of the band-edge CL peak. The two model calculations give similar results. It is not yet known whether the compositional fluctuations are simply the statistical fluctuations that occur in a random alloy or, on the other hand, are larger than random.

References

[1]   S. C. Jain, M. Willander, J. Narayan, and R. Van Overstraeten, J. Appl. Phys. **87**, 965 (2000)

[2]   I. Ho and G.B. Stringfellow, Appl. Phys. Lett. **69**, 2701 (1996)

[3]   K. Osamura, S. Naka, and Y. Murakami, J. Appl. Phys. **46**, 3432 (1975)

[4]   R. Singh, D. Doppalapudi, T.D. Moustakas, and L.T. Romano, Appl. Phys. Lett. **70**, 1089 (1997)

[5]   E.L. Piner, N.A. El-Masry, S.X. Liu, and S.M. Bedair, in *Nitride Semiconductors,* edited by F.A. Ponce, S.P. DenBaars, B.K. Meyer, S. Nakamura, and S. Strite (Mater. Res. Soc. Proc. 482, Warrendale, PA, 1998), p. 125

[6]   N. A. El-Masry, E. L. Piner, S. X. Liu, and S. M. Bedair, Appl. Phys. Lett. **72**, 40 (1998)

[7]   B. Monemar, J. P. Bergman, J. Dalfors, G. Pozina, B.E. Sernelius, P.O. Holtz, H. Amano, and I. Akasaki, MRS Internet J. Nitride Semicond. Res. **4**, 16 (1999)

[8]   N. A. Shapiro, Piotr Perlin, Christian Kisielowski, L. S. Mattos, J. W. Yang, Eicke, and R. Weber, MRS Internet J. Nitride Semicond. Res. **5**, 1 (2000)

[9]   L.H. Robins, J.T. Armstrong, R.B. Marinenko, M.D. Vaudin, C.P. Bouldin, J.C. Woicik, A.J. Paul, W.R. Thurber, K.E. Miyano, C.A. Parker, J.C. Roberts, S.M. Bedair, E.L.Piner, M.J. Reed, N.A. El-Masry, S.M. Donovan, and S.J. Pearton, submitted to Phys. Rev. B15

[10]   M. Leszczynski, T. Suski, J. Domagala, and P. Prystawko, in *Properties of Group III Nitrides*, ed. by J. H. Edgar, Electronic Materials Information Service (EMIS) Datareviews Series (Institution of Electrical Engineers, London, 1999), p. 6

[11]   Q. Guo, N. Itoh, H. Ogawa, and A. Yoshida, Jpn. J. Appl. Phys. **34**, 4653 (1995)

[12]   N.J. Jeffs, A.V.Blant, T.S. Cheng, C.T. Foxon, C. Bailey, P.G. Harrison, J.F.W. Mosselmans, and A.J. Dent, in *Wide-Bandgap Semiconductors for High Power, High Frequency and High Temperature,* edited by S. DenBaars, J. Palmour, M. Shur, and M. Spencer (Mater. Res. Soc. Proc. 512, Warrendale, PA, 1998), p. 519

[13]   R.W. Martin, P.G. Middleton, K.P. O'Donnell, and W. Van der Stricht, Appl. Phys. Lett. **74**, 263 (1999)

[14]   C. A. Parker, J. C. Roberts, S. M. Bedair, M. J. Reed, S. X. Liu, N. A. El-Masry, and L. H. Robins, Appl. Phys. Lett. **75**, 2566 (1999)

[15]   T.L. Tansley and C.P. Foley, J. Appl. Phys. **59**, 3241 (1986)